Time Transfer Experiments Based on BDS Code Observations

Wejin Qin, Jia Liu, Xuhai Yang
Chinese Academy of Science National Time Service Center Xi'an, China

***Abstract*—The Chinese BeiDou Navigation Satellite System (BDS) is assuredly going to be used for remote clock comparisons and time dissemination, along with its primary use as a global navigation system. In its current preliminary stage, the performance of the BDS Common View (CV) time transfer has been investigated because of its simplicity and ease of operation. In the study presented here, four laboratories are involved in the experiments of BDS time transfer. First, the characteristics of the BDS code measurements are analysed, and it is verified that elevation-dependent delay variations exist in the BDS code-based measurements. When empirical correction values are applied, the quality of the BDS B2 code measurements is comparable to similar measurements that use GPS or Galileo signals. All the results of the four baselines show that using the BDS geostationary satellite signals results in the largest noise. We conclude that it is more suitable to restrict signals from the other BDS satellites, particularly the Europe to Asia long baselines.**

Keywords—BeiDou Navigation Satellite System (BDS); time transfer; common view; code bias correction; Allan deviation

I. INTRODUCTION

The first application of Global Navigation Satellite System (GNSS) signals for time transfer was by way of the GPS Common View (CV) in the early 1980s[1]. Subsequently, for overcoming the limitations of GPS CV, such as decreased precision with an increasing baseline, the GPS All in View (AV) has been proposed as a better approach. This approach became feasible with the availability of the IGS precise clock and orbital products. After the application of the proper corrections, the precision of the time transfer is uncorrelated with the distance between the two sites that are involved[2]. Later, the existence of receivers capable of phase and code measurements in time laboratories made the GPS Precise Point Position (PPP) for time transfer possible[3]. The floating ambiguity resolution of the GPS PPP is adequate for frequency comparisons of all commercial clocks, while it is insufficient to compare the high-performance fountains at the level of their claimed uncertainty. The integer-ambiguity PPP (IPPP) has been developed by allowing for frequency comparisons within 10E-16[4].

GLONASS was the second GNSS that contributed to the generation of the International Atomic Time (TAI), and GLONASS CV or GPS AV combined with GLONASS CV has been in use for over two decades[5]. Preparations are ongoing to include the processing of signals from the newly built BeiDou Navigation Satellite System (BDS) and from the European Galileo in the generation of TAI and Coordinated Universal Time (UTC). Some evolutions concerning BDS and Galileo have been published recently[6-8]. The first absolute calibration of BDS signal delays in a receiver was announced by the French Space Agency (Centre National d'Etudes Spatiales, CNES)[9].

This contribution addresses the initial use of BDS for time scale comparisons. The development of BDS was done in three steps. Currently[10], BeiDou-2 consists of five satellites in a geo-stationary orbit (GEO), six in an inclined geo-synchronous orbit (IGSO) and three in a "more standard" GNSS-type orbit (MEO), while BeiDou-3 consists of five test satellites and two MEO satellites[11]. BDS has been officially providing an open service for the Asia-Pacific region since 2012. The optimal observation area is currently in East Asia and Australia, which is a result of the orbital coverage of the BeiDou-2 satellites that have been launched up to now. The full operational capability is planned for 2020. At that time, having merged BeiDou-2 and BeiDou-3, the BDS constellation will consist of three GEO satellites, twenty-four MEO satellites and three IGSO satellites[12]. The BeiDou system time (BDT) is related to UTC through the UTC(NTSC) achieved at the National Time Service Center (NTSC)[13].

Similar to GLONASS, in the prevailing preliminary stage, it seems worth studying the performance of BDS CV links because of their processing simplicity and ease of operation. Experiments on BDS CV were carried out along Europe - Asia baselines. These results and a comparison with GPS time transfer between the same sites are presented in this paper.

Section 2 introduces the GNSS CV processing strategy. Section 3 describes the experimental data. Section 4 discusses the details of the BDS code measurements, analyses the code bias variations that were observed for two frequencies and later compares the results of BDS and GPS time transfer. Section 5 summarizes the findings and concludes with an outlook.

II. METHODS/RESULTS

The computation procedure is based on the analysis of the measured pseudo ranges at the 30 s sampling interval that are combined into conventional 13-minute tracks following the CGGTTS V2E format[14]. A weighting scheme is used for

individual satellite observations based on the elevation angle. The reciprocal is adopted for averaging the result of the time comparison in each link. The redundancy of the data can ensure the robustness and reliability of the time link. The chosen elevation cut-off angle is 10 degrees. station antenna coordinates were determined from GPS PPP solutions and are held fixed. The dry component of the troposphere delay is corrected by the Saastamoinen model. The Multi-GNSS broadcast ephemeris is available at the BKG data centre[15].

This paper only refers to the BeiDou-2 satellite. The satellites of BeiDou-2 are emitting signals on three frequencies: B1 (1,561.098 MHz), B2 (1,207.14 MHz) and B3 (1,268.52 MHz). The satellite orbit is fitted on a sequence of orbit parameters, the satellite clock is fitted with a second-order polynomial. The time group delay of BDS B1 and B2 are both aligned to the B3, with the form of B1-B3 and B2-B3. All the dual signal employed in the paper is listed here, The paper are B1I and B2I for BDS, C1W and C2W for GPS, E1 and E5a for Galileo.The satellites of BeiDou-2 are emitting signals on three frequencies: B1 (1,561.098 MHz), B2 (1,207.14 MHz) and B3 (1,268.52 MHz). The satellite orbit is fitted on a sequence of orbital parameters, and the satellite clock is fitted with a second-order polynomial. The time group delay of BDS B1 and B2 are both aligned to B3, with the form of B1-B3 and B2-B3. All the dual signals employed in the paper are listed here, which are B1I and B2I for BDS, C1W and C2W for GPS, and E1 and E5a for Galileo.

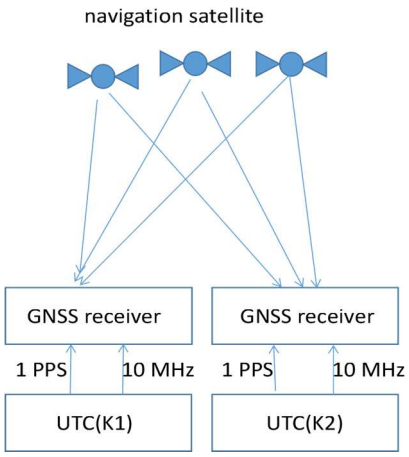

Fig.1. The schematic diagram of the GNSS CV time transfer

III. STATION NETWORK SETUP FOR THE GNSS CV TIME TRANSFER

PTB has an important status in the time and frequency metrology in Europe and plays an active role in multi-GNSS time transfer. PT09 and PT11, which are two Septentrio PolaRx4TR receivers capable of receiving BDS signals, have been operational since August, 2017. In this paper, all the time transfer experiments are obtained with PTB as the reference. Data from the five stations that are listed in Table 1 are used in the time transfer campaign, and all 5 stations are equipped with the same receiver as the PTB. Such receivers have the advantage of being able to perfectly synchronize the internal clock to an external signal source. Using identical receivers avoids potential additional bias from mixed-receiver types in the time transfer results[15]. The length of the baselines is 0.285 km, 454 km, 2182 km and 7170 km.

The investigation period was selected as DOY 238-246, 2017. All the stations are connected to a local UTC realization, namely, UTC(PTB) for PTB, UTC(ORB) for BRUX, UTC(ROA) for ROAP, and UTC(NTSC) for NTP3. Table 1 contains some further information.

Lab	Continent	Antenna type
PTB	Europe	NOV750.R4
PTB	Europe	LEICA AR25
ORB	Europe	JAVRINGANT
ROA	Europe	LEICA AR25
NTSC	Asia	SEPCHOKE_MC

The time scales compared are all derived from active hydrogen masers, and the quality of the Choke-Ring antennas in terms of multipath suppression should also be similar.

IV. ANALYSIS OF BDS CV TIME TRANSFER

As explained before, BDS signals are transmitted on three carrier frequencies, which are designated B1, B2 and B3. Currently, B1I and B2I are used for the open service. The BDS observations made by the multi-GNSS geodetic receiver are reported in the Receiver INdependent EXchange format (3.02)[16] ,and the observation type C2I represents B1I and C7I represents B2I. Ionosphere-free combinations allow for the removal of the ionosphere delays to the first order (99.9% of the effect), but the measurement noise is amplified as well. The coefficients of the ionosphere-free combinations are computed with the following equation and are listed in Table 2.

$$coe1 = \frac{f_1^2}{f_1^2 - f_2^2},\ coe2 = \frac{f_2^2}{f_1^2 - f_2^2} \qquad (1)$$

It is well known that the coefficients of the Galileo ionosphere-free combination are smaller than those of GPS and BDS. The coefficients are determined by the largest square difference between the two frequencies involved. The further the frequencies are apart, the smaller the coefficients and thus the smaller the increase in the measurement noise.

TABLE II. COEFFICIENTS FOR EACH GNSS

	GPS		Galileo		BDS	
fre	L1	L2	E1	E5a	B1	B2
	1575.42	1227.60	1575.42	1176.45	1561.09	1207.14
coe	2.546	1.546	2.261	1.261	2.487	1.487

Unlike GPS and Galileo, BDS code measurements still have some elevation-dependent Code Bias Variations (CBVs)[17]. A quantitative estimate of the CBVs can be obtained by a multi-path (MP) combination of measured pseudoranges, which is expressed by the combination of a single-frequency code and dual-frequency phase measurements[17].

$$MP_{Bi} = P_{Bi} - \Phi_{Bi} + \frac{2\lambda_{Bi}^2}{\lambda_{Bj}^2 - \lambda_{Bi}^2}(\Phi_{Bj} - \Phi_{Bi}) \quad (2)$$

where P_{Bi} is the pseudo-range, ϕ_{Bi} is the carrier phase, λ_{Bi} is the wavelength of the signal B_i, and i represents a carrier frequency.

For investigating the relationship between the MP and elevation, the linear correlation is described with the Pearson formula[18].

$$\rho_{MP,E} = \frac{N \cdot \sum MP \cdot E - \sum MP \sum E}{\sqrt{(N \cdot \sum MP^2 - (\sum MP)^2)}\sqrt{(N \cdot \sum E^2 - (\sum E)^2)}} \quad (3)$$

where E represents the elevation angle, and N represents the number of the elevation angle. The correlation coefficient $\rho_{MP,E}$ varies from [−1, 1]. The absolute value of $\rho_{MP,E}$ is closer to 1 for BDS, which implies a stronger relationship between MP and E. A value of 0 would imply that there is no linear correlation between MP and E.

The satellite C07 is invisible in ROA (Spain). For comparison, the satellites G05 (GPS) and E05 (Galileo) have been included in the analysis shown in Fig. 2. Here, C6-C10 are BDS IGSO and C11-C14 are BDS MEO.

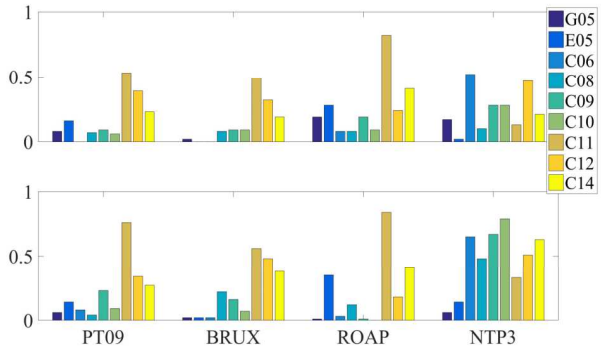

Fig.2. Absolute value of the Pearson coefficient (3) for the two frequencies used for a ionosphere-free linear combination.

It can be noted in Fig.2 that $\rho_{MP,E}$ for BDS MEO signals is larger than that of IGSO signals, whereas GPS and Galileo signals have negligible values only. The correlation of BDS B2 signals is larger than that of BDS B1 signals, which is a result of the lower B2 frequency. The $\rho_{MP,E}$ for IGSO is particularly large in NTP3. This result can be explained by the distribution and the high elevation orbits of IGSO satellites seen at NTSC. Overall, it is evident that such systematic error exists in the BDS code measurements. However, the reason is hard to explain, and perhaps the cause is on-board the BeiDou-2 satellites. Fortunately, the cause seems to be not obvious for all the available signals of the newer BeiDou-3 satellites[19].

Different kinds of models have been proposed to correct for the CBV of BeiDou-2 satellites[20-22]. Lou and Zou both selected the stations inside China for their study, whereas Wanninger selected the stations from those participating in the Multi-GNSS EXperiment (MGEX) that are distributed globally. In the present work, the Wanninger model is employed. IGSO and MEO bias corrections have been calculated by Wanninger, with a node separation of 10 degrees in frequencies B1 and B2[23-27]. In other words, each frequency has 10 code correction values. A linear interpolation is computed between the empirical values for obtaining the practical corrections corresponding to the prevailing elevation angles. The BDS MP time series of the uncorrected and corrected data are plotted in Fig.3 - 6 for one Asian station and one European station, including two frequencies and two types of satellites.

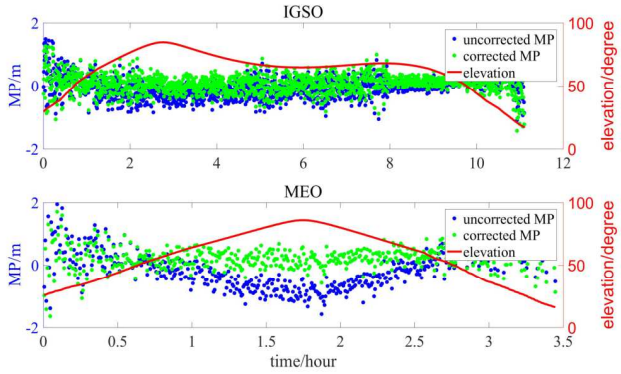

Fig.3. MP B1 time series of observations of BDS IGSO and MEO satellites in station NTP3

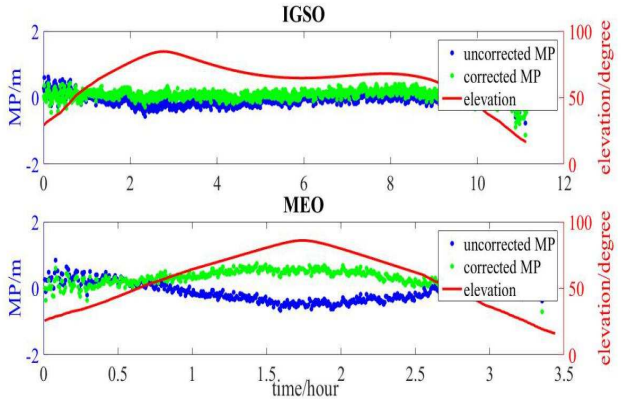

Fig.4. MP B2 time series of observations of BDS IGSO and MEO satellites in station NTP3

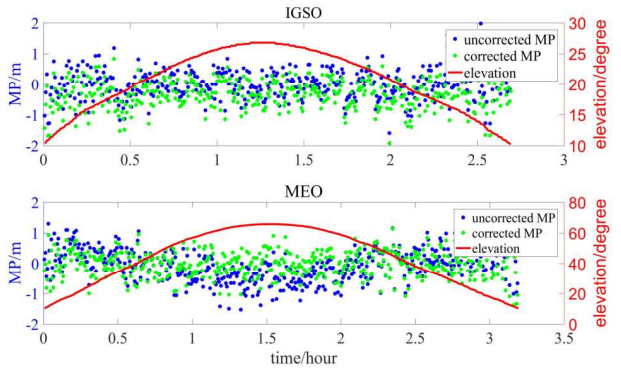

Fig.5. MP B1 time series of IGSO and MEO in station PT09

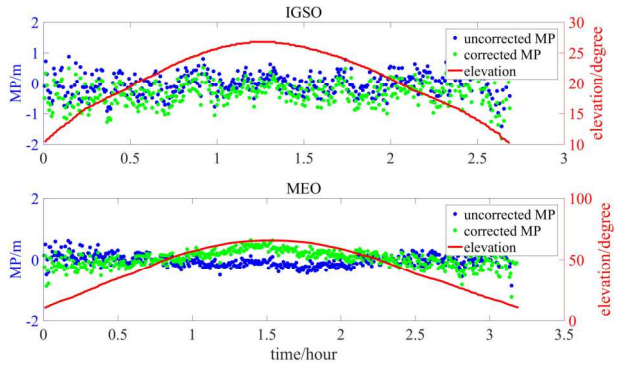

Fig.6. MP B2 time series of observations of BDS IGSO and MEO satellites in station PT09

NTP3 has an optimal location, which is capable of observing IGSO over the complete elevation range and of receiving more data. In Fig.3 and 4, before the correction, the MP observable for both frequencies is obviously elevation-dependent, especially at higher elevations, and PT09 reflects the same problem as that of NTP3. In Figures 5 and 6, after the correction, the elevation-dependent biases disappeared in the MP observable. The MP observable is now distributed evenly. The improvement of the MEO signal reception is more apparent than that of the IGSO signals, which is in accordance with the Pearson coefficient (Fig.2).

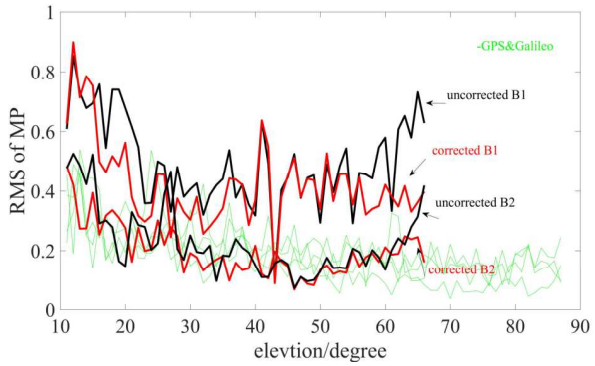

Fig.7. RMS of GNSS MEO MP values as a function of the elevation angle with each GNSS at station PT09, DOY 237/2017

Fig.7 shows the MP RMS of various signals as a function of elevation angle, including GPS (L1 and L2), Galileo (E1 and E5a), and the uncorrected and corrected BDS (B1 and B2). After correction, the tendency of the BDS RMS curve is in accordance with the MP characteristic in which it decreases at higher elevations. More importantly, the BDS B2 code data are comparable to those of GPS and Galileo. However, there is still a need for some improvement in the CBV model because it is not quite effective at each elevation angle.

To characterize the BDS time transfer capabilities, the common clock experiment excludes the influence of the time and the frequency source. PT09 and PT11 are separated by approximately 285 m, and the two receivers are equipped with the same clock signal. The pulse per second (1 PPS) and 10 MHz signals that serve as the time and frequency references are split using pulse and frequency distribution amplifiers. The experimental setup for the local common-clock baselines at PTB is depicted in Fig.8.

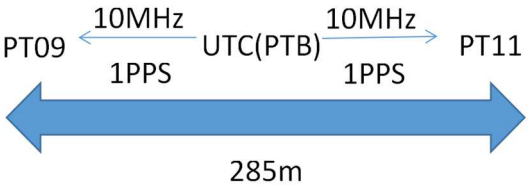

Fig. 8. The setup for the common-clock baseline at PTB

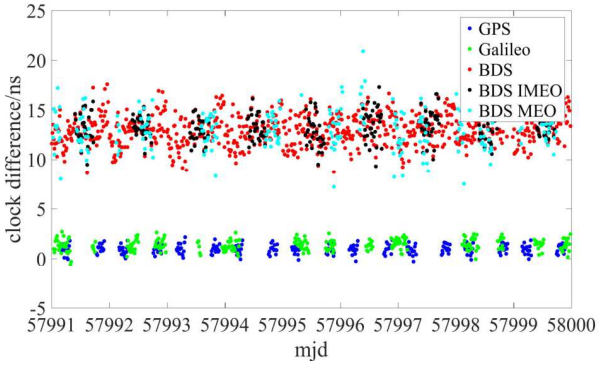

Fig.9. Clock difference between common-clock links PT09-PT11

When a common-clock experiment is performed, theoretically, the clock difference should be close to zero. Here, the BDS signal delay calibration is beyond our consideration. As a result, some offsets remain in the results, as well as measurement noise and MP noise. In Fig.9, BDS represents all the visible satellites. The GPS and Galileo satellites are MEOs; thus, they are out of view for several hours per day. As a consequence, the result is non-continuous when restricted to a single specific satellite. We estimate the frequency instability for the common-clock comparison with Allan deviations (ADEV) instead of using Time Deviation (TDEV) in order to effectively avoid some excursions caused by the data gap[9].

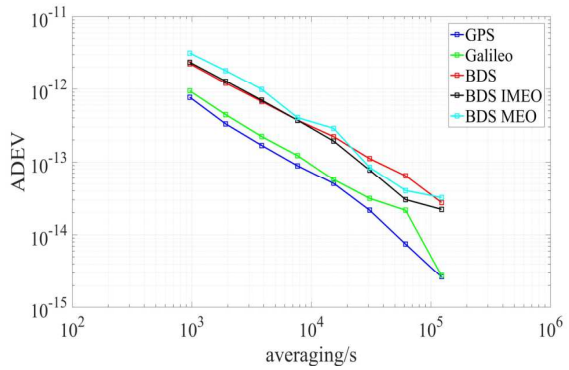

Fig.10. Instability of the clock difference PT09-PT11 in a common-clock link at PTB for the different signals used

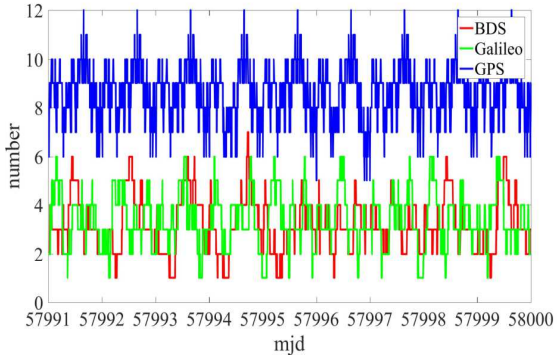

Fig.11. The number of satellites in common view for each GNSS at PTB

In Fig.10, we report five distinct ADEV plots that indicate the GPS link as the most stable of all the links. This result is because of the GPS global constellation in which the GPS satellites are evenly distributed all over the world. At least 6 satellites contribute to the weighted average (Fig.11), but the total is mostly 7-8 satellites. The more satellites that are in view, the better the stability that can be achieved. The frequency stability of the Galileo link is superior to the BDS link, as more Galileo satellites are visible in the European region. For BDS links, BDS IMEO (IGSO&MEO combined) provides better stability than the other two kinds of combinations. For BDS, we provide three combinations: BDS complete (red), MEO only (cyan) and MEO plus IGSO (black). The GEO C05 can be observed in PTB at the extreme low elevation angle of 16°. The BDS combination has only a marginal difference from the BDS MEO+IGSO combination due to the low elevation angle of GEO C05 and its small weight in the combination of results. IGSO is a dynamic satellite when it refers to the time transfer solution. IGSO increases the number of satellites and also temporarily contributes signals from a high elevation angle.

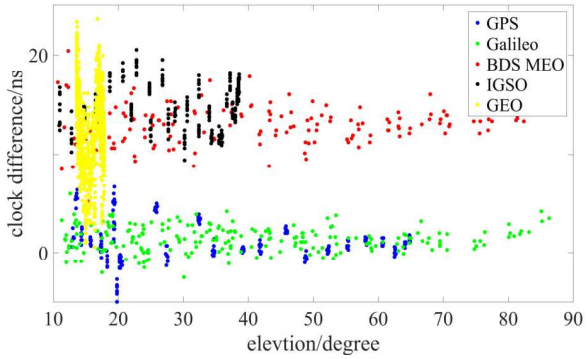

Fig.12. The relationship between the CV results of BDS, Galileo and GPS, and the satellite elevation of one satellite per type, during 9 days for the common-clock link PT09-PT11

The results of the investigations into the measurement noise are plotted in Fig.12. Each colour represents the CV result for one single satellite. The Galileo results suffer the lowest noise because of the smaller coefficient in the Galileo ionosphere-free combination, as illustrated in Table 1. When comparing MEO signals, the BDS data have the largest instability. Within BDS, GEO is much noisier than MEO and IGSO, even at the same elevation angle. The weighting solution in CV based on the elevation angle suggests that the GEO gets a reduced weight in the case that all the satellites have the same elevation angle. In the long term, when BDS is going to be completed, one may omit the GEO from any time transfer data analysis.

C.BDS TIME TRANSFER ON LONG BASELINE

Two inner-continental links and one Europe-Asia link were analysed in the context of the BDS time transfer experiment with and without code correction, and the GPS CV results are added for comparison. The achievable frequency stability can be estimated and compared from the ADEV at the average time of 960 s.

The value of MP can be considered as the indicator of the data quality. PT09 was chosen for the experiments because of generally having a smaller MP value than for PT11 – as seen in Fig.13. However, the PT11 antenna has the same quality, and its location is theoretically the more favourable one. The results of the time transfer are depicted in Fig.14. The offsets among the various types of links are due to the missing calibration of the signal delays, particularly for the BDS and Galileo signals. Therefore, the relevant information provided is the dispersion of the data points, which is a measure for the time transfer stability.

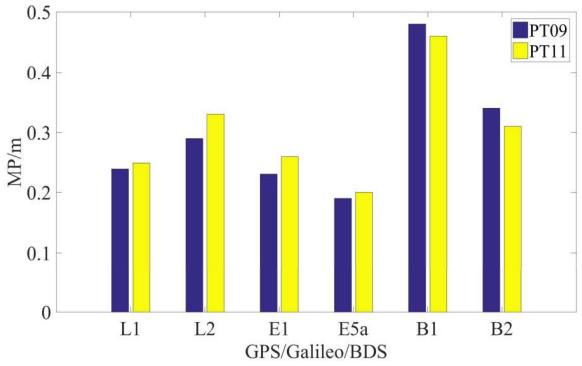

Fig.13. MP of PT09 and PT11 for signals of the three GNSSs, averaged over all satellites for 9 days.

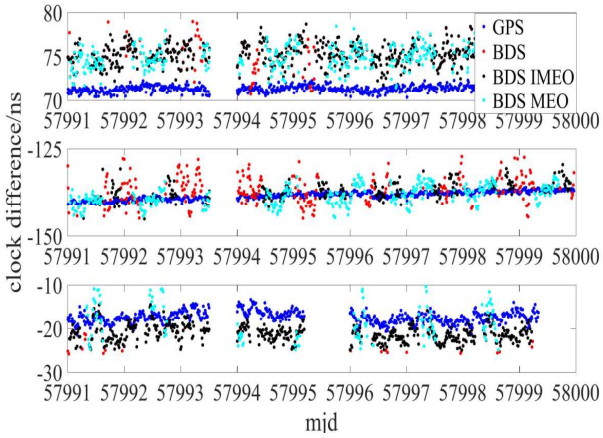

Fig.14. Clock difference for three links with four time transfer methods, from top to bottom: PT09-BRUX, PT09-ROAP, and PT09-NTP3

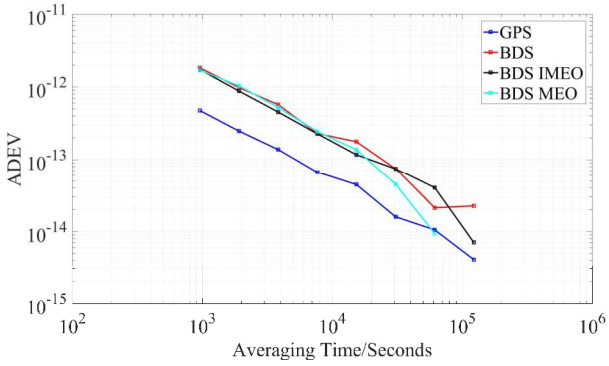

Fig.15. Allan deviations of the frequency comparison results for the link PT09-BRUX

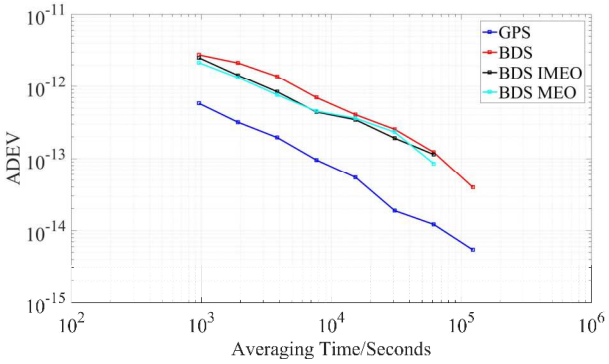

Fig.16. Allan deviations of the frequency comparison results for the link PT09-ROAP

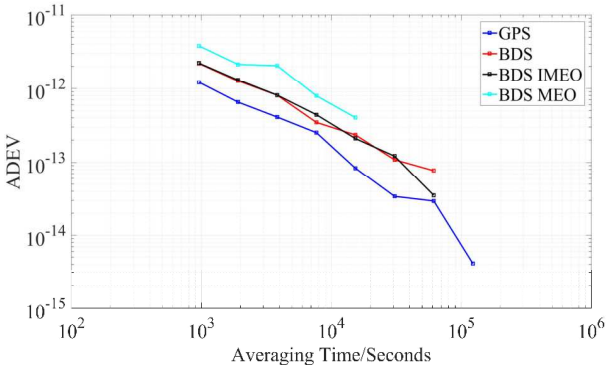

Fig.17. Allan deviations of the frequency comparison results for the link PT09-NTP3

From Fig.15-17, is can be seen that BDS IMEO is recommended for BDS time transfer, especially in the Europe-Asia links, in which redundant observations ensure the stability of the very long link. In the previous section, it was verified that GEO observations are noisier than those of other satellites. Thus, the use of GEO signals will contaminate the CV results. Hence, in the following section, we analyse the satellite-induced CBV effect on time transfer with the combination of IMEO and apply the corrections as explained in Section 4.1 for each observation.

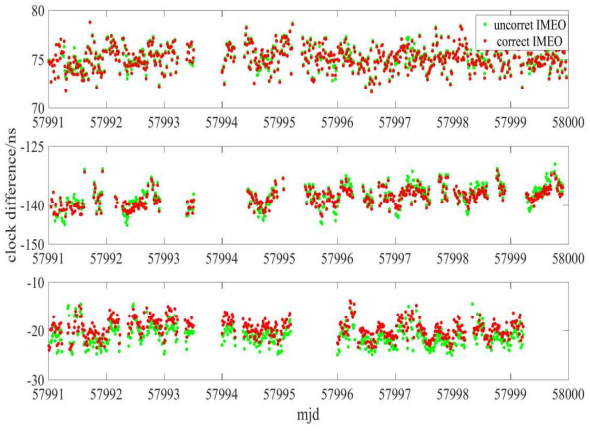

Fig.18. CBV effect on time transfer for three links– from top to bottom: PT09-BRUX, PT09-ROAP and PT09-NTP3

In Fig.18, with CBV corrections applied to the three links, the clock differences become less noisy than without correction. The effect from the BDS code bias is removed from the CV results. The noise is mitigated, regardless of whether a short baseline or a long baseline is analyzed.

In Table 3, we summarize the statistical uncertainty U_A expressed by the standard deviation (std) without correction and with correction. Here, the GPS PPP solution serves as the reference in all cases.

TABLE3. STANDARD DEVIATION OF EACH LINK

Baseline	GNSS link	uA(= std) (ns)
PTB-BRUX	uncorrected IMEO CV	1.18
	correct_IMEO CV	1.17
	GPS CV	0.41
PTB-ROA	uncorrected IMEO CV	2.57
	correct IMEO CV	1.95
	GPS CV	0.51
PTB-NTSC	uncorrected IMEO CV	2.03
	correct IMEO_CV	1.98
	GPS CV	1.25

For the three links, the U_A of the BDS CV results decreases after correction. It is well-known that the CV uA decreases with the increasing baseline, while the precision of the PTB-ROA link is nearly the same as that of PTB-NTSC. This result is attributed to the satellite coverage. A total of 75% of the CV results of the PTB-ROA link have one visible satellite during the investigation period, while less than 50% of the CV results of the PTB-NTSC link have one visible satellite.

Finally, we show the results of the investigation of the BDS CBV effect on the three links using individual satellite observations at a certain elevation angle.

Fig.19 illustrates that the BDS time transfer stability is improved after the application of the empirical values. This outcome appears to be a necessity at the moment.

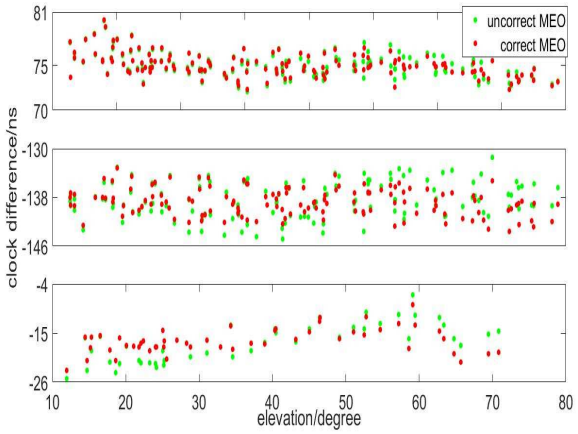

Fig.19. CBV effect of a single satellite in time transfer for three links- from top to bottom: PT09-BRUX, PT09-ROAP and PT09-NTP3

V. CONCLUSION

In this paper, first, the background of BDS was introduced. Then, we analyzed the characteristics of the BDS code measurement, and it was detected that the elevation-dependent system variations exist in the BDS code measurements B1 and B2. The bias is removed after correction, and, as we expected, the quality of the BDS B2 code measurements are comparable to those using GPS or Galileo signals. Four baselines have been analyzed when assessing the BDS performance. The suggestion is that BDS IGSO&MEO is most suitable for BDS time transfer, particularly for the Europe to Asia long links. After the correction of code bias, the CV results become smoother than before. The statistical noise of all links is obviously reduced. Hence, BDS code bias corrections should be accounted for in BDS time transfer. Currently, the third generation BDS satellites are gradually being put into service. We expect that better time transfer performance will be achieved quite soon, when global coverage with BDS signals is achieved. Sooner or later, the results of BDS time transfer will contribute to the realization of the International Atomic Time by the Bureau International des Poids et Mesures (BIPM).

Acknowledgment: The author thank PTB,ORB and ROA for sharing their data. Weijin Qin thanks the CAS Youth Innovation Promotion Association (No.2019398) and CAS Western Scholar(No.XAB2019A06)

REFERENCES

[1] D. W. Allan et al. 1983. Technical Directives for Standardization of GPS Time Receiver Software, Metrologia, 31, 69-79.

[2] BeiDou Navigation Satellite System Signal In Space Interface Control Document, Open Service Signal B1C, B2a (beta version), 2017.

[3] Gérard Petit, Zhiheng Jiang, 2008b. Precise Point Positioning for TAI Computation. International Journal of Navigation and Observation, 1–8.

[4] Gérard Petit, Amale Kanj, Sylvain Loyer, 2015. 1×10^{-16} frequency transfer by GPS PPP with integer ambiguity resolution. Metrologia, 52(2), 301~305.

[5] Guang Wei, Yuan Haibo, 2013. The Application of Smoothed Code in Beidou Common View, Lecture Notes in Electronic Engineering. V243 LNEE, 269-278.

[6] http://www.bipm.org/en/news/full-stories/2017-09-beidou.html.

[7] http://interact.beidou.gov.cn/interact/download.service?attachment=2013/12/26/20131226fe8b20aad5f34091a6f8a84b08b1c4b1.pdf.

[8] http://www.septentrio.com/

[9] I. Sesia, P. Tavella, 2008. Estimating the Allan variance in the presence of long periods of missing data and outliers. Metrologia, 45(6), S134-S142.

[10] Lambert Wanninger, Susanne Beer, 2015. BeiDou satellite-induced code bias variations: diagnosis and therapy. GPS Solution, 19, 639–648.

[11] Lou Y, Gong X, Gu S, Zheng F, Feng Y, 2017. Assessment of code bias variations of BDS triple-frequency signals and their impacts on ambiguity resolution for long baselines. GPS Solution, 21(1), 177-186.

[12] Mgex.igs.org/IGS_MGEX_Status_BDS.html#satellites.

[13] N.Nadarajah, P.Teunissen, J.-M. Sleewaegen, O. Montenbruck, 2014. The

[14] mixed-receiver BeiDou inter-satellite-type bias and its impact on RTK positioning, GPS Solution, 19(3), 57-368.

[15] P. Defraigne, C.Bruyninx, 2006. Multipath mitigation in GPS-based time and frequency transfer. 2006 EFTF Meeting, Braunschweig, Germany.

[16] Pearson K, 1895. Note on regression and inheritance in the case of two parents. Proc. R. Soc. Lond.

[17] P Defraigne, G Petit, 2015. CGGTTS-Version 2E: an extended standard for GNSS Time Transfer. Metrologia , 52(6) , 1-8.

[18] Igs.bkg.bund.de/0:/MGEX/BRDC_v3/2017/ brdm.

[19] Petit G, Jiang Z, 2008. GPS All in view time transfer for TAI computation. Metrologia, 45, 35–45.

[20] Jiang Z, Lewandowski W, 2012. Use of GLONASS for UTC time transfer. Metrologia, 49, 57-61.

[21] Jiang Z, Lewandowski W, 2009. Three Years of GLONASS Use for UTC. 44th annual Precise Time and Time Interval (PTTI) System and Applications Meeting.

[22] Wei Huang and Pascale Defraigne, 2016. BeiDou Time Transfer With the Standard CGGTTS. IEEE Trans Ultrason Ferroelectr Freq Control, 63(7), 1005-1012.

[23] Weijin Qin, et al, 2017. Common-View Time Transfer Based on Beidou Observations. The 6th International Colloquium-Scientific and Fundamental Aspects of GNSS / Galileo.

[24] Wang G, de Jong K, Zhao Q, Hu Z, Guo J, 2015. Mutipath analysis of code measurements for BeiDou geostationary satellites. GPS Solution, 19(1), 129-139.

[25] Xiaohong Zhang, Mingkui Wu, Wanke Liu, 2017. Initial assessment of the COMPASS/BeiDou-3: new-generation navigation signals. Journal of Geodesy, 91, 1225-1240.

[26] Zou X, Li Z, Li M, 2017. Modeling BDS bias variations and models assessment. GPS Solution, 21(4), 1661-1668.